

Wireless Power Transfer System with the Auxiliary Resonant Commutated Pole Converter for Reducing Radiated Emission

Rintaro Kusui
Dept. of Electrical, Electronics, and
Information Engineering
Nagaoka University of Technology
Nagaoka, Japan
kusui@stn.nagaokaut.ac.jp

Keisuke Kusaka
Dept. of Electrical, Electronics, and
Information Engineering
Nagaoka University of Technology
Nagaoka, Japan
kusaka@vos.nagaokaut.ac.jp

Hiroki Watanabe
Dept. of Electrical, Electronics, and
Information Engineering
Nagaoka University of Technology
Nagaoka, Japan
watanabe@vos.nagaokaut.ac.jp

Jun-ichi Itoh
Dept. of Electrical, Electronics, and
Information Engineering
Nagaoka University of Technology
Nagaoka, Japan
itoh@vos.nagaokaut.ac.jp

Abstract— Wireless power transfer systems improve the convenience for EV users. However, the WPT systems generate the radiated emission caused by current harmonics that interfere with wireless communications. To solve this problem, this paper proposes a WPT system with an auxiliary resonant commutated pole (ARCP) converter with selective harmonic elimination (SHE) on the primary and secondary sides. The ARCP converter suppresses the increasing switching losses on main devices, and the SHE-PWM reduces coil current harmonics components that cause radiated emissions. Furthermore, the proposed system controls a constant boost current to minimize losses in the auxiliary circuit. In this paper, the switching phases are numerically analyzed in order to eliminate the low-order harmonics voltage of the converter output voltage. Then, the operation of the proposed system is demonstrated by simulation and experiment. As a result, it is confirmed that the harmonics below the 13th order are reduced by more than 40 dB in the simulation. In addition, the experimental results with the prototype of the three-pulse SHE-PWM mention that all switching achieved zero voltage switching.

Keywords— *Wireless power transfer, Auxiliary resonant commutated pole converter, Selective harmonics elimination, Current harmonics, Radiated emission*

I. INTRODUCTION

Wireless power transfer (WPT) systems for easy and safe charging of electric vehicles (EVs) are actively studied [1-3]. The WPT system transfers power through a large air gap, resulting in weak magnetic coupling. As a result, radiated emissions are generated from the transmission coil. Radiated emissions interfere with other electronic devices or wireless communications and can adversely affect health. The International Special Committee on Radio Interference (CISPR: Comité International Spécial des Perturbations Radioélectriques) and the International Commission on Non-Ionizing Radiation Protection (ICNIRP) establish reference levels for radiated emissions from transmission coils [4-5]. In particular, the standard for the WPT system in CISPR 11 Class A Group 2 is planned to be about 30 dB stricter for low-order harmonic components [6]. For this reason, the WPT systems require a reduction of the coil current harmonics that cause the radiated emissions.

Most conventional WPT systems have a full-bridge inverter on the primary side and a diode rectifier on the secondary side as power supplies [7]. These power converters output square wave voltages that include large low-order harmonics. The square wave voltage applied to the transmission coil and compensation circuit causes currents containing harmonics to flow according to the frequency characteristics of the resonator. The transmission coils generate large leakage flux depending on the currents on coils since the magnetic coupling between coils is very low. As a result, the conventional WPT systems radiate the leakage magnetic fields with large harmonic components [2].

The WPT systems with asynchronous PWM inverters and multi-level converters, such as flying capacitor topology, have been proposed in order to reduce the low-order harmonics of the radiated emissions of the WPT systems[8-9]. The PWM and multi-level converters reduce the output voltage harmonics of the primary and secondary converters. As a result, the harmonics of radiated emissions from the transmission coils are reduced. However, almost all switching operation becomes hard-switching. Thus, the losses and surge voltages cause an increase in higher-order harmonic radiation. In addition, the asynchronous PWM induces low-frequency beat components in the output current and power. Synchronous PWM avoids the output current and output power beat components with selective harmonic elimination (SHE) [10]. However, the switching losses by hard switching and radiation noise by surges are unavoidable.

Meanwhile, an auxiliary resonant commutated pole (ARCP) converter has been proposed to reduce switching losses and radiation noise in power converters[11-12]. The ARCP converter achieves zero-voltage switching (ZVS) in all switching of the main devices by applying a resonant current to the main switches just before commutation. As a result, the ARCP converter suppresses the increase in switching losses and the surge voltages in the main switches. Thus, the ARCP converter can reduce radiated emissions. However, the authors do not know that the ACRP converter has been applied to high-frequency inverters, such as the WPT system, in order to reduce radiated emissions.

This paper proposes a WPT system that has an ARCP converter with SHE on the primary and secondary sides. The

new contribution of this paper is that the proposed system reduces switching losses by ARCP and low harmonics components of the inverter output voltage by SHE. This paper demonstrates the reduction of the coil current harmonics components by the simulation and the commutation operation under the ZVS in the proposed system by the experiment.

II. PROPOSED WPT SYSTEM

A. Circuit configuration of the proposed WPT system

Figure 1 shows the circuit configuration of the proposed system. The proposed WPT system has ARCP converters on the primary and secondary sides. The resonant capacitors of the WPT system are connected in series between the transmission coil and the ARCP converter for both the primary and secondary sides, which is called series (S-S) compensation. The ARCP converters for this system achieve ZVS by flowing a resonant current between phases in the commutation period by applying unipolar modulation. Due to this, the ARCP converter needs only one additional inductor and two auxiliary switches. In addition, the proposed system must have a short transient time to output a PWM-controlled voltage with 85-kHz fundamental frequency for the WPT. For this purpose, the ARCP of the proposed system uses only the parasitic capacitance of the main switch without the additional resonance capacitor connected in parallel with the main switch in the conventional ARCP.

B. ARCP Full-bridge converter

Figure 2 shows the output voltage and output current waveforms and the switching timing of the ARCP full-bridge converter during the commutation period. The resonant inductor L_r is charged by turning on the auxiliary switch of the ARCP just before the commutation of the main switches. The charged current discharges the charges stored in the parasitic capacitor C_r of the main devices. In this paper, the resonant inductor current i_r is minimized in order to minimize the losses of the auxiliary circuit. The inductor charging time is adjusted depending on the load current i_L to keep the constant boost current I_b . The inductor charging time t_{b1} in Fig. 2(a) and (b) is expressed as (1), and the charging time t_{b2} in (c) and (d) is expressed as (2).

$$t_{b1} = \frac{L_r |i_L + I_b|}{V_{DC}} \quad (1),$$

$$t_{b2} = \frac{L_r |I_b - i_L|}{V_{DC}} \quad (2),$$

where L_r is the inductance of the resonant inductor of the ARCP and V_{DC} is the DC link voltage. After the resonant inductor is fully charged, turning off the main device initiates resonance between the resonant inductor and the parasitic capacitor of the main device. The negative current flows on the other main switch by resonance. ZVS is achieved by turning on the main device during negative current flow.

Figure 3 shows the equivalent circuit of the ARCP converter at resonance. From Fig. 3, the resonance current i_r and the inverter output voltage v_{out} at resonance in Fig. 2(a) are expressed as

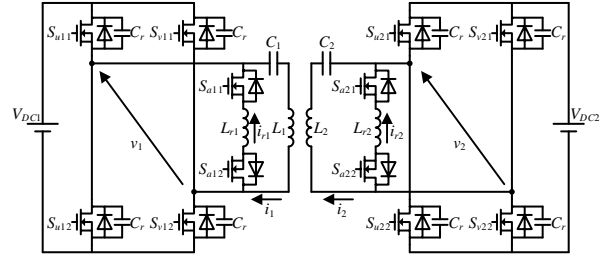


Fig. 1. Configuration of proposed wireless power transfer system.

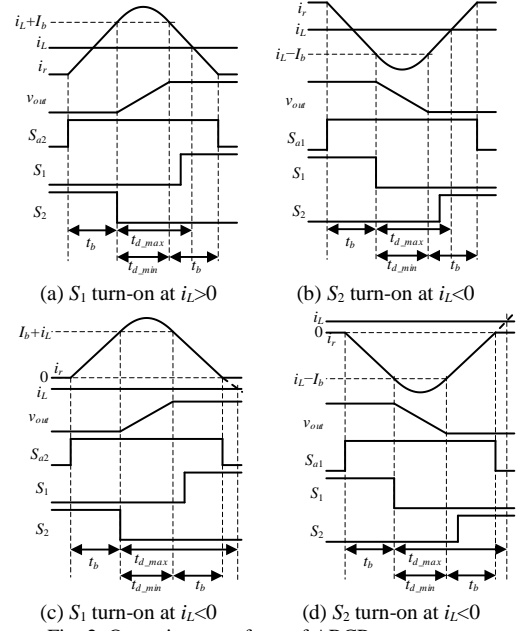


Fig. 2. Operation waveform of ARCP converter.

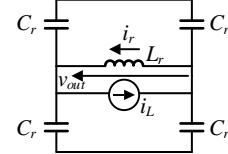


Fig. 3. Equivalent circuit when the ARCP is in resonance condition.

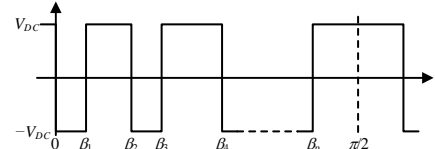


Fig. 4. p -pulse PWM waveform for Fourier series expansion (1/4 cycle).

$$i_r = I_b \cos \omega_r t + \frac{V_{dc}}{Z_r} \sin \omega_r t + I_L \quad (3),$$

$$v_{out} = Z_r I_b \sin \omega_r t - V_{dc} \cos \omega_r t \quad (4),$$

where ω_r is the resonance angle frequency of the resonance circuit. In order to achieve ZVS of the main device, i.e., to discharge the charges of the parasitic capacitors, $v_{out} = V_{DC}$ must be satisfied. From (3) and (4), the minimum time t_{d_min} to achieve ZVS is expressed as

$$t_{d_min} = \frac{1}{\omega_r} \left(\tan^{-1} \left(\frac{V_{DC}}{Z_r I_b} \right) + \sin^{-1} \left(\frac{V_{DC}}{\sqrt{V_{DC}^2 + Z_r^2 I_b^2}} \right) \right) \quad (5),$$

where Z_r is the characteristic impedance of the resonant circuit and is expressed as

$$Z_r = \sqrt{\frac{L_r}{C_r}} \quad (6).$$

The minimum time at which ZVS is achieved in Fig. 2 (b)~(d) is also calculated in the same way and agrees with (5). The parasitic diodes turn on by fully discharging the parasitic capacitors. Thus, the inductor voltage is clamped to the DC voltage. As a result, the inductor current is reduced due to a change according to the sign of the inductor voltage. The parasitic capacitor is recharged by the inductor current becoming smaller than the load current. In other words, the ZVS of the main device fails. The recharging start time t_{d_max} is expressed as

$$t_{d_max} = t_{d_min} + \frac{L_r I_b}{\omega_r V_{DC}} \quad (7).$$

C. Selective harmonics elimination

Figure 4 shows a quarter cycle of the p (p : odd) pulse PWM waveform in a half cycle of an inverter using unipolar modulation. The switching phase angle β_k must be calculated by the modulation ratio to eliminate the low-order harmonics components in the PWM waveform. The n th (n : odd) order harmonic component in the PWM waveform is calculated by Fourier series expansion of the waveform in Fig. 4 to be expressed as

$$a_n = \frac{4V_{DC}}{n\pi} \left(-1 + 2 \sum_{k=1}^p (-1)^{k+1} \cos n\beta_k \right) \quad (8),$$

where β_k is the switching phase angle of the inverter, there are p freely variable phases when the number of pulses is p . Accordingly, p equations are needed to derive all the phase angles. Since the PWM waveform contains only odd-order components, all switching phase angles are derived from the fundamental and harmonic components up to $2p-1$ order. Assuming that the amplitude of the fundamental component is unity and the harmonic components are zero, the p simultaneous nonlinear equations are expressed as

$$\begin{cases} a_1 = 1 \\ a_3 = a_5 = \dots = a_{2p-1} = 0 \end{cases} \quad (9).$$

It is impossible to solve these nonlinear simultaneous equations analytically. Thus, the on/off phase angles β_k that eliminate harmonics are solved numerically. Table 1 shows the on/off phase angles β_k when the number of pulses is three, five, and seven, and the fundamental wave amplitude is unity, respectively.

Figure 5 shows the harmonic analysis results of the SHE-PWM waveforms with switching angles in Table 1. Furthermore, it also shows the harmonic analysis results of the square wave used in most conventional WPT systems. The results of harmonic components are normalized by the fundamental component. From Fig. 5, the square wave includes many low-order harmonics. The results also show that the PWM waveform using the numerically analyzed

Table 1. Turn-on and turn-off angle for harmonics elimination.

	3 pulse	5 pulse	7 pulse
β_1	0.291601942	0.212415864	0.167133468
β_2	0.811286668	0.537036587	0.400587541
β_3	0.897609093	0.643599531	0.50383472
β_4	-	1.064356019	0.798263952
β_5	-	1.093330767	0.847657035
β_6	-	-	1.18959039
β_7	-	-	1.202551877

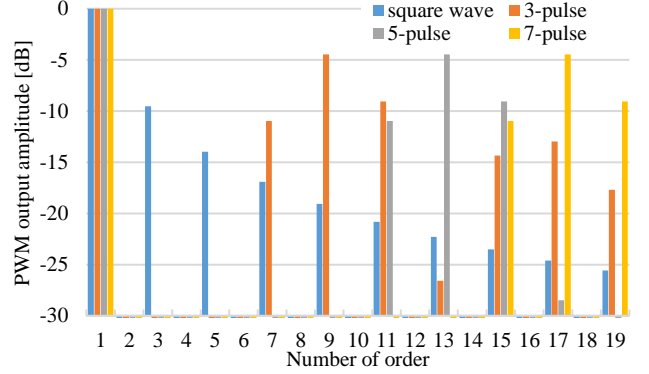


Fig. 5. Harmonics components in selective harmonics elimination PWM waveform.

Table 2. Simulation conditions.

Parameter	Symbol	Value
DC voltage	V_{DC1}, V_{DC2}	400 V
Rated output power	P_{out}	1 kW
Transmission frequency	f	85 kHz
Selfinductance	L_1, L_2	500 μ H
Resonant capacitor	C_1, C_2	7.02 nF
Coupling coefficient	k	0.3
Resonant inductor	L_r	350 nH
Parastic capacitor	C_r	100 pF
Boost current	I_b	6 A
Dead time	t_d	10.2 ns

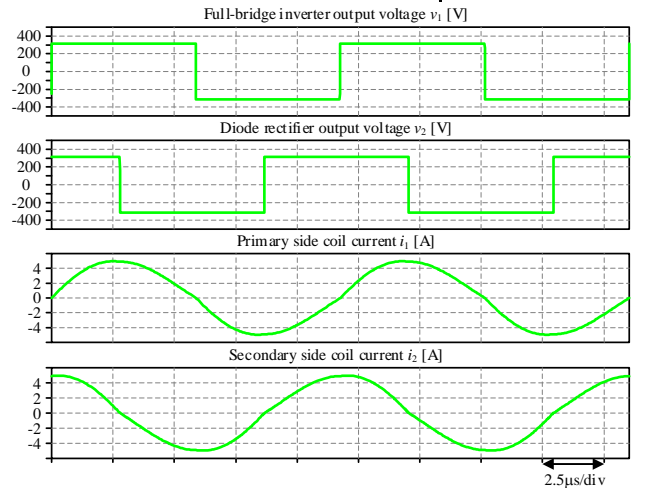


Fig. 6. Operation waveform of conventional WPT system.

switching phases has zero fifth order or lower for three pulses, ninth order or lower for five pulses, and 13th order or lower for seven pulses. This result confirms the validity of the harmonic analysis of the PWM waveform and the switching phase angle obtained from the Fourier coefficients.

III. SIMULATION RESULT

Figure 6 shows the simulation results of a conventional WPT system with a full-bridge inverter and diode rectifier. The waveforms show the output voltage and current of the primary and secondary power converters, respectively. Fig. 6 indicates that the WPT system transmits power under resonant conditions because of the unity power factor. However, it is seen that the current on both the primary and secondary side are distorted due to the harmonics in the current.

Figure 7 shows the operating waveforms of the proposed system, and Table 2 shows the simulation conditions. The seven-pulse PWM is applied in the simulation, and the on/off phase angles in Table 1 are used. Fig. 7 shows the primary and secondary ARCP converter output voltage and the transmission coil current, respectively. The simulation results show that the ARCP converter outputs seven pulses in a half cycle. In addition, the fundamental power factor from the primary and secondary ARCP outputs is also nearly unity respectively. In other words, it is seen that the WPT system operates in the resonance condition.

Figure 8 shows the operating waveforms of the ARCP converter in the proposed system and the enlarged waveforms at switching on both the primary and secondary sides. They show the drain-source voltage and the switching signal of the U-phase upper arm switch, the output current, and the current in the resonant inductor. The boost current of the proposed system is controlled at a constant to minimize the resonant inductor current while achieving ZVS. From Fig. 8, it is seen

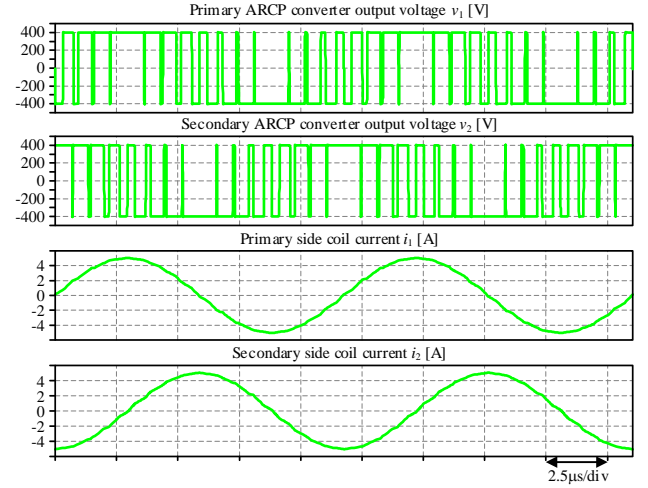
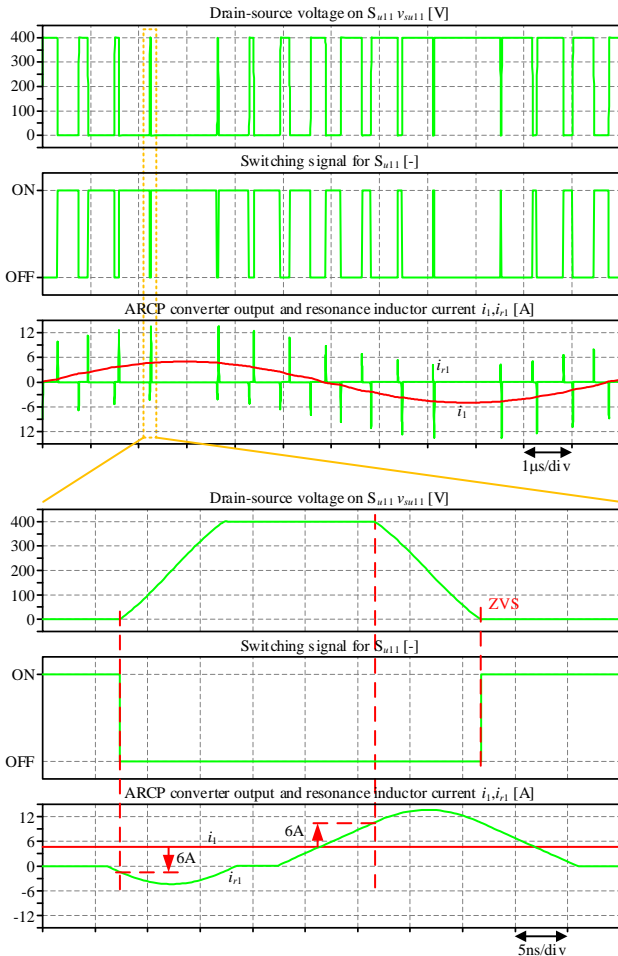


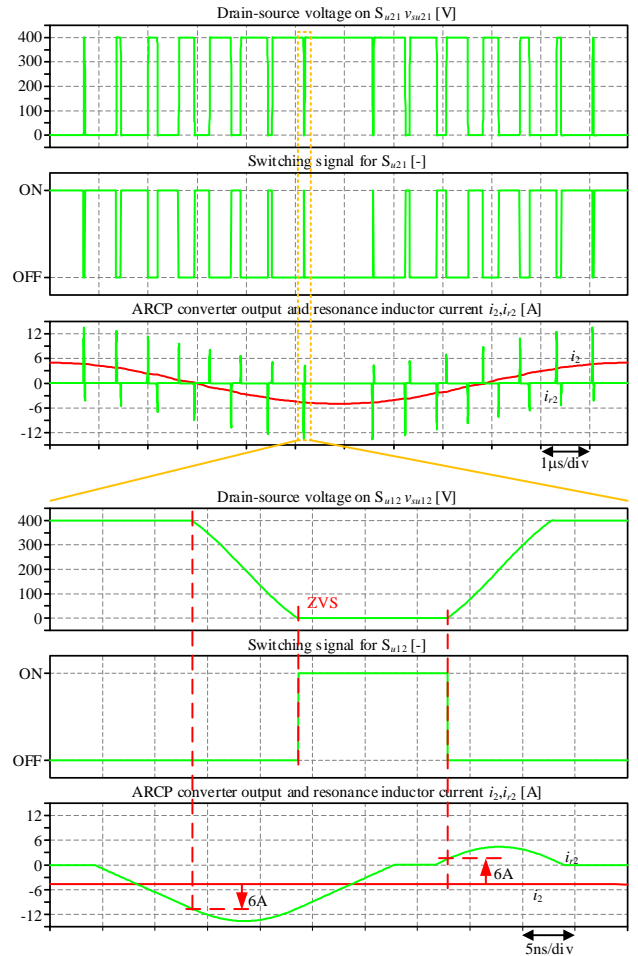
Fig. 7. Operation waveform of proposed WPT system.

that the resonant inductor current changes with the output current. In addition, the resonant inductor current at the start of the commutation is always 6 A greater than the load current, i.e., the boost current is controlled at a constant level of 6 A. Due to this, it is confirmed that all switching achieves ZVS.

Figure 9 shows the harmonic analysis results of the primary and secondary currents, and Table 3 shows the odd-order harmonic components under the 13th harmonic. The current harmonics when using a two-level inverter are also shown for comparison. The inverter DC voltage in the two-

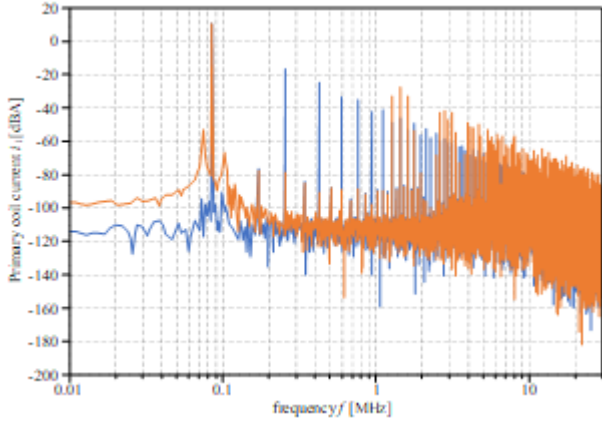


(a) primary side ARCP converter

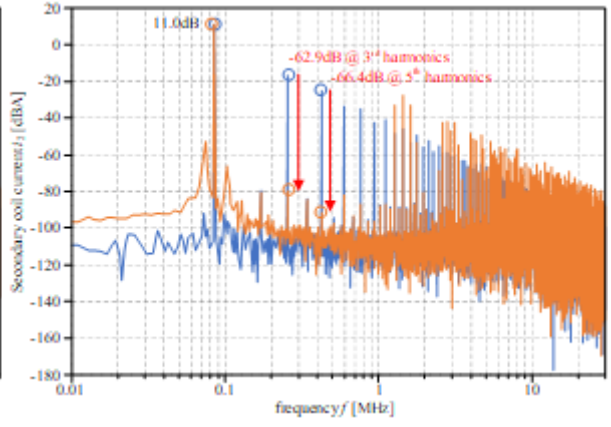


(b) Secondary side ARCP converter

Fig. 8. Operation waveform of ARCP converter and enlarged waveform at turn-on and turn-off for S_{u11}



(c) Primary side ARCP converter operation waveform



(d) Secondary side ARCP converter operation waveform

Fig. 9. Harmonics analysis for the primary and secondary side coil current in simulation.

Table 3 Analysis results of current harmonics at odd-order components

(a) Primary side coil current

Configuration	Number of order						
	1st	3rd	5th	7th	9th	11th	13th
Conv. [dBA]	11.0	-16.7	-24.9	-33.4	-35.0	-42.3	-41.1
Prop. [dBA]	11.0	-78.5	-90.3	-88.6	-88.3	-97.8	-89.6

(b) secondary side coil current

Configuration	Number of order						
	1st	3rd	5th	7th	9th	11th	13th
Conv. [dBA]	11.0	-16.7	-24.9	-33.4	-35.0	-42.3	-41.1
Prop. [dBA]	11.0	-78.5	-90.3	-88.6	-88.3	-97.8	-89.6

level inverter is multiplied by $\pi/4$ so that the fundamental components of the output voltage are equal. Fig. 9 indicates that the fundamental components of the output current are the same in both systems. In contrast, the harmonic components are reduced by approximately 40dB from the 3rd to the 13th order components on both the primary and secondary sides. Note that the components below the 13th order cannot be eliminated because the switching phases of the analytical solution and the experimental waveform are different due to the dead time and commutation period of the ARCP converter. In addition, the current harmonics at uneliminated components above the 13th order increase. However, the higher harmonic components are significantly attenuated according to the frequency characteristics of the transmission coil and the compensation circuit. In other words, they are not expected to contribute to a significant increase in the radiated emissions.

IV. EXPERIMENTAL RESULT

The ARCP converter must control the boost current to match the switching timing of the main device. However, it is expected to be more difficult due to the higher resonance frequency in this paper when the main switch operates at a high frequency. Hence, in order to confirm the feasibility of the ARCP converter, the commutation operation is verified experimentally, and the fundamental characteristics are confirmed.

Figure 10 shows the operating waveforms of the WPT system with the ARCP converter. Three-pulse PWM is applied for the experiment, and the DC voltage and the resonance inductance are changed from the simulation conditions to 100 V and 3 μ H, respectively. The waveforms mention the resonator voltages and transmission coil currents of the primary and secondary sides, respectively. From the operating waveforms, the power factor of each power source is approximately unity. Accordingly, it is confirmed that the WPT system transmits power in the resonance condition.

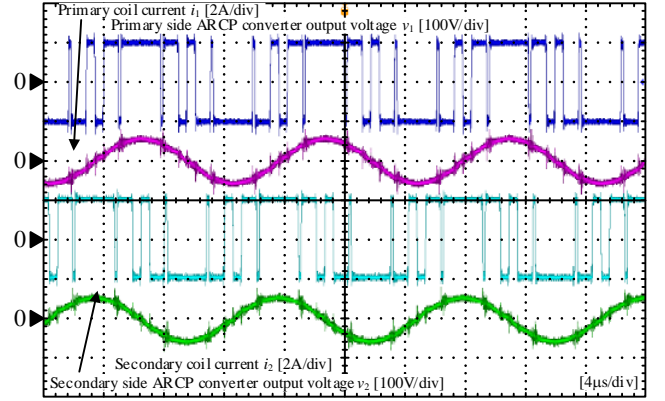


Fig. 10. Operation waveform of WPT system.

Figure 11 shows the operating waveforms of the primary and secondary ARCP converters and their enlarged views. The waveforms are the output voltage of the ARCP converter, the gate-source voltage and drain current of the U-phase upper arm switch, and the resonant inductor current. From Fig. 8, it is seen that a negative current flows on the U-phase upper arm switch S_{u11} by applying a boost current to the resonant inductor just before the S_{u11} turns on. That is, the ZVS of the main switch is confirmed. Note that there is a ringing in the resonant inductor current after the commutation is complete. The ringing current causes the resonance between the resonant inductor and the parasitic capacitor of the auxiliary switch excited by the recovery of the auxiliary switch.

V. CONCLUSION

This paper proposed a configuration of a WPT system using an ARCP converter with a synchronous SHE-PWM on the primary and secondary sides to reduce the coil current harmonics. The on/off phase angle of the synchronous PWM was numerically analyzed for seven-pulse PWM. It was verified by simulation that the proposed system reduces the harmonics of the coil currents. The results revealed that the proposed system reduced the 13th-order and lower harmonics of the transmission coil current harmonics by approximately

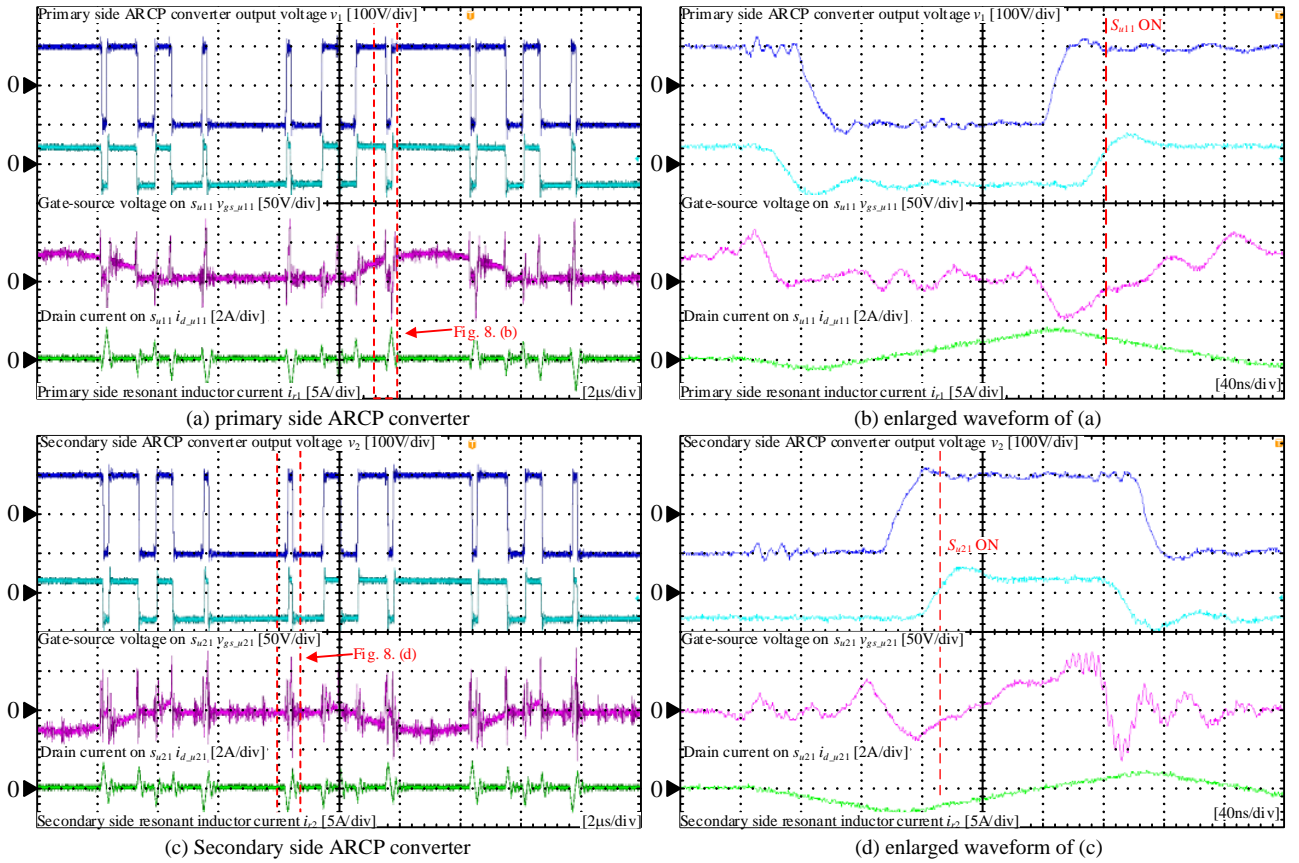


Fig. 11. Operation waveform of ARCP converter.

40 dB. In addition, the commutation operation of the proposed system was verified by prototype with the three-pulse SHE-PWM. Furthermore, it was confirmed that ZVS was achieved at all switching. In future work, harmonic analysis of coil currents and radiated emissions will be measured in experiments.

REFERENCES

- [1] Keisuke Kusaka, Rintaro Kusui, Jun-ichi Itoh, Daisuke Sato, Tetsu Shijo, Shuichi Obayashi, Masaaki Ishida: "A 22kW Three-phase Wireless Power Transfer System in Compliance with CISPR 11 and ICNIRP 2010," *IEEE Journal of Industry Applications*, Vol. 11, No. 4, pp. 594-602, (2022)
- [2] H. Sumiya, E. Takahashi, N. Yamaguchi, K. Tani, S. Nagai, T. Fujita, H. Fujimoto: "Coil Scaling Law of Wireless Power Transfer Systems for Electromagnetic Field Leakage Evaluation for Electric Vehicles," *IEEE Journal of Industry Applications*, Vol. 10, No. 5, pp. 589-597 (2021)
- [3] Ryohei Okada, Ryosuke Ota, Nobukazu Hoshi: "Novel Soft-Switching Active-Bridge Converter for Bi-directional Inductive Power Transfer System," *IEEE Journal of Industry Applications*, Vol. 11, No. 1, pp. 97-107 (2022)
- [4] Ministry of Internal Affairs and Communications, Japan, "Inquiry of technical requirements for wireless power transfer system for EVs in technical requirements for wireless power transfer system in standards of International Special Committee on Radio Interference (CISPR)", (2015)
- [5] International Commission on Non-Ionizing Radiation Protection (ICNIRP): "Guidelines for Limiting Exposure to Electromagnetic Fields (100 kHz to 300 GHz)," *Health Phys.*, Vol. 118, No. 5, pp. 483-524 (2020)
- [6] N. Misawa : " Situation of EMC Limit Level of WPT for EV in CISPR," 2019 JSAE Annual Congress (Spring) Latest Trend of EV Charging System, No. 20194438, pp.15-20 (2019)
- [7] K. Kusaka, J. Itoh: "Development Trends of Inductive Power Transfer Systems Utilizing Electromagnetic Induction with Focus on Transmission Frequency and Transmission Power," *IEEE Journal of Industry Applications*, Vol. 6, No. 5, pp. 328-339 (2017)
- [8] S. Nagai, T. Fujita, H. Sumiya, O. Shimizu, H. Fujimoto, "Reduction of Magnetic Field by Low-order Harmonics in Magnetic Resonant Wireless Power Transfer System Using High-frequency Switching," *IEEE Trans. on Industry Applications*, Vol. 142, No. 5, pp. 385-392 (2022)
- [9] R. Kusui, K. Kusaka, J. Itoh, "WPT system with flying-capacitor converter on both primary and secondary side for current harmonics reduction," *PE/PSE/SPC2023*, SPC-23-148 (2023)
- [10] I. Takahashi, T. Takahashi, "Digital Control Method of PWM Inverter Using ROM," *The trans. of the Institute of Electrical Engineers of Japan. B*, Vol. 96, No. 2, pp. 97 (1976)
- [11] W. McMurray, "Resonant snubbers with auxiliary switches," *IEEE Trans. on Industry Applications*, Vol. 29, No. 2, pp. 355-362 (1993)
- [12] R. W. De Doncker and J. P. Lyons: "The auxiliary resonant commutated pole converter," *IEEE Industry Applications Society Annual Meeting*, Vol.2, pp. 1228-1235 (1990)